

Experimental demonstration of tunable graphene-polaritonic hyperbolic metamaterial

Jeremy Brouillet,¹ Georgia T. Papadakis,^{1, a)} and Harry A. Atwater¹

Thomas J. Watson Laboratories of Applied Physics, California Institute of Technology, California 91125, USA

(Dated: 10 July 2019)

Tuning the macroscopic dielectric response on demand holds potential for actively tunable metapotonics and optical devices. In recent years, graphene has been extensively investigated as a tunable element in nanophotonics. Significant theoretical work has been devoted on the tuning the hyperbolic properties of graphene/dielectric heterostructures, however, until now, such a motif has not been demonstrated experimentally. Here we focus on a graphene/polaritonic dielectric metamaterial, with strong optical resonances arising from the polar response of the dielectric, which are, in general, difficult to actively control. By controlling the doping level of graphene via external bias we experimentally demonstrate a wide range of tunability from a Fermi level of $E_F = 0$ eV to $E_F = 0.5$ eV, which yields an effective epsilon-near-zero crossing and tunable dielectric properties, verified through spectroscopic ellipsometry and transmission measurements.

Spectral tunability is key for controlling light-matter interactions, critical for many applications including emission control, surface enhanced spectroscopy, sensing, and thermal control. Particularly in the subwavelength range, tuning plasmonic resonances has been essential in controlling color, typically achieved by controlling the size of plasmonic nanoparticles, antennas and metamaterials¹⁻⁴. In obtaining a large range of spectral tunability, it is preferable to operate near an optical resonance rather than a broadband plasmonic response. Nevertheless, it is in general easier to tune a broadband optical response rather than a resonant one since resonances in nanophotonics typically entail subwavelength-scale geometrical features.

From a very wide range of recently investigated metamaterials and heterostructures for spectral control, particular emphasis has been given to hyperbolic media, due to enhanced light-matter interactions arising from a larger range of wavenumbers available for propagating modes⁵. These media are in generally uniaxial and support a hyperbolic frequency dispersion given by the equation^{3,6-8}

$$\frac{k_x^2 + k_y^2}{\epsilon_o} + \frac{k_z^2}{\epsilon_e} = \frac{\omega^2}{c^2} \quad (1)$$

where ϵ_o and ϵ_e refer to the ordinary (in-plane) and extraordinary (out-of-plane) dielectric permittivity, respectively. Due to the different sign in ϵ_o and ϵ_e , upon fixing the frequency ω , the isofrequency diagram of the relevant electromagnetic modes opens up into a hyperbola, giving rise to a very large density of optical states, promising for waveguiding⁹, emission engineering and Purcell enhancement^{1,2,10} thermal photonics¹¹, lasing¹², and imaging^{13,14}. Particularly, near the epsilon-near-zero frequency crossing of either ϵ_o or ϵ_e , many exciting phenomena can be supported, the most prominent of which is light propagation with near-zero phase advance¹⁵⁻¹⁷.

There has been significant effort in frequency-tuning of the optical response of hyperbolic metamaterials^{6,18-20}. For this, particular interest holds the case of graphene, a well-studied monolayer material for electronics²¹ and in infrared photonics²². Namely, the dielectric properties of graphene can be dynamically tuned via optical pumping²³, or with electrostatic modulation of its carrier concentration with field-effect gating^{24,25}, often targeting tunable plasmonic properties^{26,27}. The high degree of localization of graphene plasmons, together with the dielectric tunability of graphene provides a promising platform for investigating tunable graphene-based hyperbolic metamaterials. There has already been considerable theoretical effort in the past decade to understand the properties of tunable graphene metamaterials²⁸⁻³², with significant focus on the potential of tuning hyperbolic properties of graphene/dielectric planar heterostructures^{6,33-35}. There have previously been experimental demonstrations of graphene-based hyperbolic media^{36,37}, nevertheless, the reported properties have remained fixed at the time of fabrication. No post-fabrication way to control the dielectric permittivity tensor (ϵ_o and ϵ_e in Eq. 1) has been reported until now.

Gating graphene when integrated with dielectric layers is difficult due to graphene's two-dimensional nature with weak out-of-plane Van der Waals bonds that yield poor adhesion to most dielectric substrates. Furthermore, large-area graphene sheets on the order of mm²'s with gate-induced tunability are needed to perform metamaterial optical measurements at infrared frequencies. Exfoliated flakes are generally limited to sizes of 10s of μm , so large-area graphene samples grown by chemical vapor deposition and subsequently transferred from their growth substrates, are necessary. Additionally, deposition of large-area thin dielectric layers on graphene is challenging. Films prepared by electron-beam evaporation exhibit thermal stress-induced delamination³⁸. Films grown by atomic layer deposition (ALD) with an H₂O precursors exhibit difficulty in bonding to chemically-inert hydrophobic graphene³⁹, whereas ozone-based ALD processes oxidize graphene.

Here, we discuss how we overcome these challenges and are, thus, able to tune a graphene-based hyperbolic metama-

^{a)}Present address: Department of Electrical Engineering, Ginzton Laboratory, Stanford University, California 94305, USA; gpapadak@stanford.edu; Electronic mail: gpapadak@stanford.edu

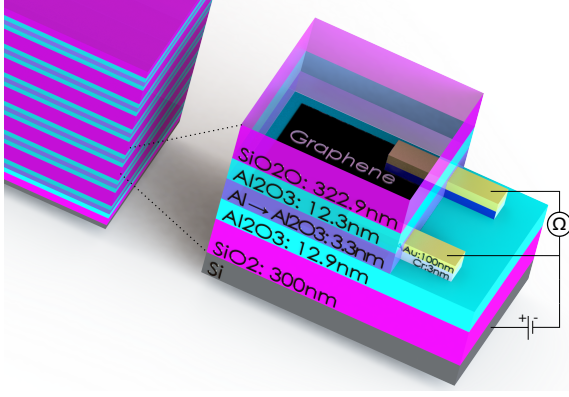


FIG. 1. Left: Schematic of a theoretical metamaterial stack. Right: Schematic of the fabricated individual device. The layers: Lightly-doped silicon substrate, thermally-grown SiO₂, Al₂O₃, transferred chemical-vapor deposited (CVD) graphene, Al₂O₃, and plasma-enhance chemical vapor deposition SiO₂. The thin layers of Al₂O₃ are necessary for the feasibility of the fabrication. The thick SiO₂ contribute to the majority of the dielectric response. Contacts are added to gate and measure the resistance of the graphene. The graphene is tuned by gating against the back silicon substrate.

material unit cell for a wide range of doping levels in graphene translating to a Fermi level that ranges from $E_F = 0$ eV to $E_F = 0.5$ eV, without dielectric breakdown. Previous theoretical proposals have considered non-dispersive dielectric materials^{6,33–35}, thereby yielding a broadband hyperbolic response. By contrast, here, we consider a polaritonic dielectric material, namely SiO₂. The polaritonic resonances that all polar materials exhibit at infrared frequencies, at their Reststrahlen band, are typically not tunable, as they constitute a fundamental material property. Nevertheless, we show here that, upon the integration of graphene, it is feasible to actively tune these polaritonic resonances. Graphene provides a tunable character to the in-plane response of the composite graphene/SiO₂ heterostructure, and its plasmonic nature assigns a hyperbolic frequency region near the polar resonance of SiO₂, at a free-space wavelength of 20 μm . We are therefore able to experimentally observe, through multi-angle spectroscopic ellipsometry and transmittance measurements, a tunable epsilon-near zero permittivity along the in-plane direction near the surface phonon polaritonic resonance while leaving the out-of-plane response unchanged (due to the two-dimensional nature of graphene), thereby yielding a widely tunable hyperbolic response.

The metamaterial under consideration is depicted in Fig. 1, and is composed of a graphene monolayer sandwiched in between two SiO₂ layers of thickness 300 nm. The alumina (Al₂O₃) layers depicted in Fig. 1 have thickness 0.5 nm and are placed to prevent poor graphene adhesion. Particularly, a viable dielectric deposition method was developed consisting of functionalization of the surface by deposition of trimethylaluminum (TMA)⁴⁰ or an aluminum nucleation layer⁴¹ to create a seed layer for additional deposition. A suitably thin layer of aluminum is needed so that it can fully oxidize and not compromise the electrical gat-

ing of the graphene. We found that deposition of Al₂O₃ via plasma-enhanced chemical vapor deposition (PECVD) resulted in reduced thermal stress and avoided delamination. The graphene is grown by chemical vapor deposition (CVD) and transferred onto the thermal oxide, whereas the top SiO₂ film is deposited by plasma-enhanced chemical vapor deposition (PECVD). The thickness of the film layers were measured by both a thin film analyzer and visible ellipsometry with a qualitative agreement of 2nm. Lithographically-defined patterns were used to deposit 3nm/100nm of Cr/Au contacts on the graphene layer, and were used to gate the graphene monolayer against the silicon substrate, which serves as the back-side contact for field-effect tuning.

Since the composite in Fig. 1 is extremely subwavelength to infrared light, one can homogenize it and assign an effective in-plane and out-of-plane dielectric response, namely ϵ_o and ϵ_e ⁸. The two-dimensional nature of graphene leaves the out-of-plane response unaffected, therefore in the out-of-plane direction, this metamaterial behaves to far-field radiation effectively as bulk SiO₂. By striking contrast, by electrostatically tuning the graphene carrier we can shift the epsilon-near-zero point of ϵ_o , and therefore control the hyperbolicity of the heterostructure as shown in Fig. 2.

In estimating the Fermi level to which we can actively tune the doping level in graphene, we use a capacitor model based on the materials between the gate and the applied voltage⁴².

$$E_f = 0.031 \sqrt{V - V_{\text{Dirac}}}. \quad (2)$$

Experimentally, the location of the Dirac peak was determined via measuring change in sheet resistance. Furthermore, we use the Kubo formula⁴³ calculate the sheet conductance σ from the E_f of graphene. This value can be used to compute the transfer matrix for graphene⁴⁴.

$$\overleftrightarrow{G} = \begin{bmatrix} 1 & 0 \\ 4\pi\sigma/c & 0 \end{bmatrix}$$

We utilize the transfer matrix approach⁴⁵, accounting for graphene via \overleftrightarrow{G} , and obtain the complex scattering amplitudes of the fields at different Fermi levels E_F . In these calculations, fabrication and material imperfections are removed by having, a priori, measured experimentally the individual layer thicknesses and optical constants of all thin films in the metamaterial, with ellipsometry. For example, in Fig. 2(a) and (b) we show the experimentally determined dielectric permittivity of the top and bottom SiO₂ films shown in Fig. 1, where their small differences are expected since the top SiO₂ is deposited via PECVD whereas the bottom one is thermally grown. The scattering amplitudes are fed into previously developed parameter retrieval approaches⁸, from which we obtain an effective uniaxial tensorial dielectric permittivity $\epsilon = \text{diag}(\epsilon_o, \epsilon_o, \epsilon_e)$ that characterizes the metamaterial composite. This process is repeated at different gating voltages V , in other words for different Fermi levels E_F .

By taking spectroscopic ellipsometry measurements of the full metamaterial stack of Fig. 1, we perform an ellipsomet-

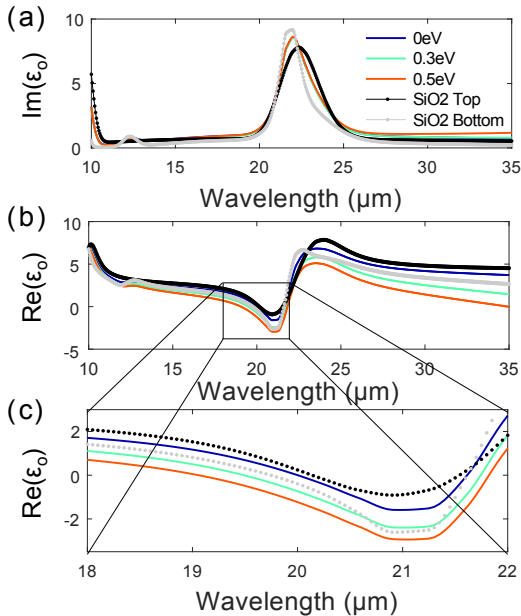


FIG. 2. Ellipsometrically derived ϵ_0 for the graphene/SiO₂ metamaterial of Fig. 1, under applied bias, for three different Fermi levels E_F . Grey and black curves correspond to the homogeneous dielectric permittivity of the bottom and top ϵ_0 films, respectively. (a) Imaginary part, and (b) real part. (c) Inset showing the epsilon-near-zero regime of ϵ_0 at different E_F 's.

ric fitting where we use the effective dielectric permittivity $\epsilon = \text{diag}(\epsilon_0, \epsilon_0, \epsilon_e)$ as a model to fit to the experimental data, namely the ellipsometric observables Ψ and Δ . In Fig. 2(a) and (b) we show the imaginary and real part of the ellipsometrically-derived in-plane permittivity ϵ_0 , at different Fermi levels E_F . We note that the out-of-plane effective permittivity ϵ_e is not tunable as described above, and therefore is omitted. There resonant character of ϵ_0 near the regime of 20 μm is attributed to the surface phonon polaritonic resonance of SiO₂ at this wavelength, nevertheless this resonance has now become tunable via incorporation of a monolayer-thick graphene sheet in between SiO₂ films. As can be clearly seen in 2(c), by gradually tuning the Fermi level of graphene from $E_F = 0$ eV (blue curves) to $E_F = 0.3$ eV (green curves) to $E_F = 0.5$ eV, we redshift the infrared response of the metamaterial by approximately a micron, i.e. from a near-zero crossing at 20 μm under no bias to 19 μm under large applied bias. Redshifting is expected as a response of applied bias because the electrostatic doping induces additional charge carriers in the graphene sheet, hence making the composite medium more metallic.

In addition to spectroscopic ellipsometry, we perform Fourier-transform infrared spectroscopy (FTIR) to measure the sample transmission, and compare with the results of spectroscopic ellipsometry shown above, derived based on initial parameter retrieval-based derivation of $\epsilon = \text{diag}(\epsilon_0, \epsilon_0, \epsilon_e)$. Electrostatically gating the graphene induces changes in the transmission of the composite metamaterial, as shown in Fig. 3. Namely, as mentioned above, gating the graphene mono-

layer makes the composite metamaterial more metallic and, therefore, less transmissive, as shown with the colormap in Figs. 3(b) and (c). The dips near the wavelengths of 16 μm and 20 μm correspond to the two surface phonon polariton resonances of SiO₂, where the material absorbs resonantly, resulting in low transmittance. We note that, experimentally, graphene exhibits hysteresis, which is attributed to defects induced by the deposition of the aluminum layer, resulting in the discrepancies between experiment and theory. As the graphene is tuned, the Dirac peak shifts in the direction of applied bias, causing the sample to experience a reduced E_F , giving qualitative experimental agreement with theory without fitting parameters as can be seen in Fig. 3(c).

To further illustrate the epsilon-near-zero shifting and the resonant nature of the in-plane dielectric response of this metamaterial, i.e. ϵ_0 , in Fig. 4 we show the relative change in dielectric permittivity, i.e. $\Delta\epsilon = 100 \times (\epsilon_{0,V=0} - \epsilon_{0,V}) / \epsilon_{0,V=0}$, for two different applied bias corresponding to $E_F=0.2$ eV and to $E_F=0.4$ eV, with blue and red color, respectively. These calculations were performed using the experimentally derived values for the optical properties and thicknesses of the constitutive components of the metamaterial, as described above. Near the surface phonon resonance of SiO₂ at 20 μm , significant tuning of the real part of ϵ_0 is observed, coming from the epsilon-near-zero tuning, which shifts by approximately 1 micron. Bearing in mind that the out-of-plane response

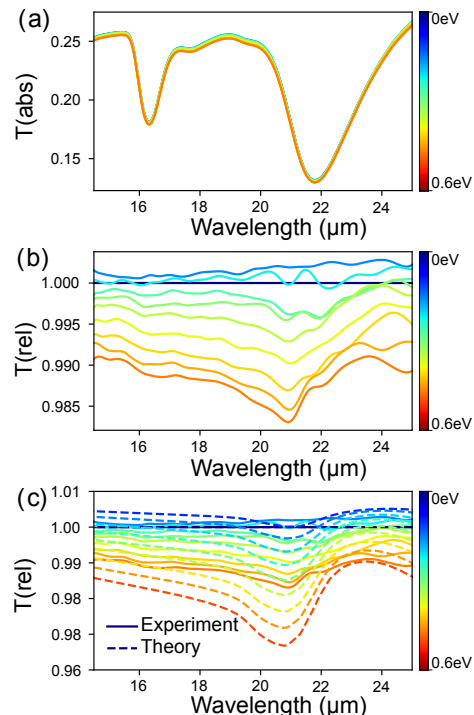


FIG. 3. (a) Absolute FTIR transmission over a range of Fermi levels. (b) Experimental data normalized to $E_F=0$, the Dirac point. (c) Experiment compared with theory, based on ellipsometric fits the thickness and optical properties constituent layers. Normalized to $E_F=0$. Deviations arise due to hysteresis of the graphene induced by charge trapping.

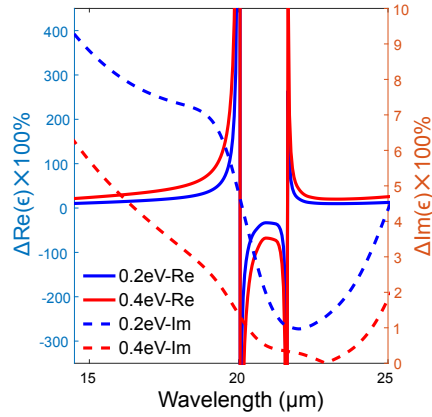


FIG. 4. Relative change of ϵ_0 with applied bias for $E_F = 0.2$ eV (blue curves) and $E_F = 0.4$ eV (red curves), where solid curves (left y-axis) correspond to real parts and dashed curves correspond to imaginary parts (right y-axis).

of this metamaterial (ϵ_e in Eq. 1) is not tunable due to the two-dimensional nature of graphene, as explained above, the change in sign of ϵ_0 on the left axis in Fig. 4 corresponds to a topological transition of the isofrequency surface of this metamaterial.

In summary, we have experimentally demonstrated a graphene/polaritonic dielectric metamaterial with tunable epsilon-near-zero permittivity response. By tuning the Fermi level of graphene by 0.5 eV, we observe a shift of 1 μm in the near-zero response. Although previous theoretical proposals have focused on non-dispersive dielectric materials between graphene monolayers, here we showed that utilizing the polar response of dielectrics at infrared frequencies benefits tunability, and additionally provides means of tuning constitutive material properties of polar dielectrics and semiconductors, by incorporating graphene. Ellipsometry was used to determine the optical properties (dielectric response and thickness) of the constituent materials, and, based on effective parameter retrievals that homogenize the metamaterial, we experimentally characterized the full metamaterial stack. FTIR transmission measurements agree with our ellipsometric results, where transmission reduction is directly attributed to electrostatically induced charges in graphene and to epsilon-near-zero tuning.

ACKNOWLEDGMENTS

This work was supported by U.S. Department of Energy (DOE) Office of Science Grant No. DE-FG02-07ER46405 (G.T.P. and H.A.A.). JB acknowledges support from a National Science Foundation Graduate Research Fellowship under Grant No. 1144469. G.T.P. acknowledges support from the TomKat Postdoctoral Fellowship in Sustainable Energy at Stanford University.

- ¹D. Lu, J. J. Kan, E. E. Fullerton, and Z. Liu, “Enhancing spontaneous emission rates of molecules using nanopatterned multilayer hyperbolic metamaterials,” *Nature nanotechnology* **9**, 48 (2014).
- ²J. Zhou, A. F. Kaplan, L. Chen, and L. J. Guo, “Experiment and theory of the broadband absorption by a tapered hyperbolic metamaterial array,” *ACS photonics* **1**, 618–624 (2014).
- ³Z. Jacob, J.-Y. Kim, G. V. Naik, A. Boltasseva, E. E. Narimanov, and V. M. Shalaev, “Engineering photonic density of states using metamaterials,” *Applied physics B* **100**, 215–218 (2010).
- ⁴J. A. Schuller, E. S. Barnard, W. Cai, Y. C. Jun, J. S. White, and M. L. Brongersma, “Plasmonics for extreme light concentration and manipulation,” *Nature materials* **9**, 193 (2010).
- ⁵D. R. Smith, W. J. Padilla, D. Vier, S. C. Nemat-Nasser, and S. Schultz, “Composite medium with simultaneously negative permeability and permittivity,” *Physical review letters* **84**, 4184 (2000).
- ⁶A. Poddubny, I. Iorsh, P. Belov, and Y. Kivshar, “Hyperbolic metamaterials,” *Nature Photonics* **7**, 948 (2013).
- ⁷D. Smith and D. Schurig, “Electromagnetic wave propagation in media with indefinite permittivity and permeability tensors,” *Physical Review Letters* **90**, 077405 (2003).
- ⁸G. T. Papadakis, P. Yeh, and H. A. Atwater, “Retrieval of material parameters for uniaxial metamaterials,” *Physical Review B* **91**, 155406 (2015).
- ⁹V. E. Babicheva, “Long-range propagation of plasmon and phonon polaritons in hyperbolic-metamaterial waveguides,” *Journal of Optics* **19**, 124013 (2017).
- ¹⁰C. L. Cortes, M. Otten, and S. K. Gray, “Ground-state cooling enabled by critical coupling and dark entangled states,” *Physical Review B* **99**, 014107 (2019).
- ¹¹S.-A. Biehs, M. Tschikin, and P. Ben-Abdallah, “Hyperbolic metamaterials as an analog of a blackbody in the near field,” *Phys. Rev. Lett.* **109**, 104301 (2012).
- ¹²A. Fang, T. Koschny, and C. M. Soukoulis, “Lasing in metamaterial nanostuctures,” *Journal of optics* **12**, 024013 (2010).
- ¹³Z. Liu, H. Lee, Y. Xiong, C. Sun, and X. Zhang, “Far-field optical hyperlens magnifying sub-diffraction-limited objects,” *Science* **315**, 1686–1686 (2007).
- ¹⁴D. S. Weile, “Electromagnetic metamaterials: Physics and engineering explorations (engheta, n. and ziolkowski, rw; 2006)[book review],” *IEEE Antennas and Propagation Magazine* **49**, 137–139 (2007).
- ¹⁵R. Maas, J. Parsons, N. Engheta, and A. Polman, “Experimental realization of an epsilon-near-zero metamaterial at visible wavelengths,” *Nature Photonics* **7**, 907 (2013).
- ¹⁶A. M. Mahmoud and N. Engheta, “Wave-matter interactions in epsilon-and-mu-near-zero structures,” *Nature Communications* **5**, 5638 (2014).
- ¹⁷N. Engheta, “Pursuing near-zero response,” *Science* **340**, 286–287 (2013).
- ¹⁸G. T. Papadakis and H. A. Atwater, “Field-effect induced tunability in hyperbolic metamaterials,” *Phys. Rev. B* **92**, 184101 (2015).
- ¹⁹J. A. Roberts, S.-J. Yu, P.-H. Ho, S. Schoeche, A. L. Falk, and J. A. Fan, “Tunable hyperbolic metamaterials based on self-assembled carbon nanotubes,” *Nano Letters* **19**, 3131 (2019).
- ²⁰L. Lu, R. E. Simpson, and S. K. Valiyaveedu, “Active hyperbolic metamaterials: progress, materials and design,” *Journal of Optics* **10**, 103001 (2018).
- ²¹K. S. Novoselov, A. K. Geim, S. Morozov, D. Jiang, M. Katsnelson, I. Grigorieva, S. Dubonos, Firsov, and AA, “Two-dimensional gas of massless dirac fermions in graphene,” *nature* **438**, 197 (2005).
- ²²D. R. Andersen, “Graphene-based long-wave infrared tm surface plasmon modulator,” *JOSA B* **27**, 818–823 (2010).
- ²³V. Ryzhii, M. Ryzhii, and T. Otsuji, “Negative dynamic conductivity of graphene with optical pumping,” *Journal of Applied Physics* **101**, 083114 (2007).
- ²⁴A. Vakil and N. Engheta, “Transformation optics using graphene,” *Science* **332**, 1291–1294 (2011).
- ²⁵M. Polini, R. Asgari, G. Borghi, Y. Barlas, T. Pereg-Barnea, and A. MacDonald, “Plasmons and the spectral function of graphene,” *Physical Review B* **77**, 081411 (2008).
- ²⁶E. Hwang and S. D. Sarma, “Dielectric function, screening, and plasmons in two-dimensional graphene,” *Physical Review B* **75**, 205418 (2007).
- ²⁷V. W. Brar, M. S. Jang, M. Sherrott, J. J. Lopez, and H. A. Atwater, “Highly confined tunable mid-infrared plasmonics in graphene nanores-

- onators,” *Nano letters* **13**, 2541–2547 (2013).
- ²⁸J. Linder and K. Halterman, “Graphene-based extremely wide-angle tunable metamaterial absorber,” *Scientific reports* **6**, 31225 (2016).
- ²⁹A. Andryieuski and A. V. Lavrinenko, “Graphene metamaterials based tunable terahertz absorber: effective surface conductivity approach,” *Optics express* **21**, 9144–9155 (2013).
- ³⁰H. Xiong, Y.-B. Wu, J. Dong, M.-C. Tang, Y.-N. Jiang, and X.-P. Zeng, “Ultra-thin and broadband tunable metamaterial graphene absorber,” *Optics express* **26**, 1681–1688 (2018).
- ³¹S. Zainud-Deen, A. Mabrouk, and H. Malhat, “Frequency tunable graphene metamaterial reflectarray,” in *2017 XXXIInd General Assembly and Scientific Symposium of the International Union of Radio Science (URSI GASS) (IEEE, 2017)* pp. 1–4.
- ³²A. Al Sayem, A. Shahriar, M. Mahdy, and M. S. Rahman, “Control of reflection through epsilon near zero graphene based anisotropic metamaterial,” in *8th International Conference on Electrical and Computer Engineering (IEEE, 2014)* pp. 812–815.
- ³³I. V. Iorsh, I. S. Mukhin, I. V. Shadrivov, P. A. Belov, and Y. S. Kivshar, “Hyperbolic metamaterials based on multilayer graphene structures,” *Physical Review B* **87**, 075416 (2013).
- ³⁴M. A. Othman, C. Guclu, and F. Capolino, “Graphene–dielectric composite metamaterials: evolution from elliptic to hyperbolic wavevector dispersion and the transverse epsilon-near-zero condition,” *Journal of Nanophotonics* **7**, 073089 (2013).
- ³⁵B. Janaszek, A. Tyszka-Zawadzka, and P. Szczepański, “Tunable graphene-based hyperbolic metamaterial operating in sclu telecom bands,” *Optics express* **24**, 24129–24136 (2016).
- ³⁶Y.-C. Chang, C.-H. Liu, C.-H. Liu, S. Zhang, S. R. Marder, E. E. Narimanov, Z. Zhong, and T. B. Norris, “Realization of mid-infrared graphene hyperbolic metamaterials,” *Nature communications* **7**, 10568 (2016).
- ³⁷S. Dai, Q. Ma, M. K. Liu, T. Andersen, Z. Fei, M. D. Goldflam, M. Wagner, K. Watanabe, T. Taniguchi, M. Thiemens, F. Keilmann, G. C. A. M. Janssen, S.-E. Zhu, P. Jarillo-Herrero, M. M. Fogler, and D. N. Basov, “Graphene on hexagonal boron nitride as a tunable hyperbolic metamaterial,” *Nature nanotechnology* **10**, 682 (2015).
- ³⁸D. Q. McNerny, B. Viswanath, D. Copic, F. R. Laye, C. Prohoda, A. C. Brieland-Shoultz, E. S. Polsen, N. T. Dee, V. S. Veerasamy, and A. J. Hart, “Direct fabrication of graphene on sio 2 enabled by thin film stress engineering,” *Scientific reports* **4**, 5049 (2014).
- ³⁹J. S. Park, K. D. Kihm, H. Kim, G. Lim, S. Cheon, and J. S. Lee, “Wetting and evaporative aggregation of nanofluid droplets on cvd-synthesized hydrophobic graphene surfaces,” *Langmuir* **30**, 8268–8275 (2014).
- ⁴⁰B. Lee, G. Mordi, M. Kim, Y. Chabal, E. Vogel, R. Wallace, K. Cho, L. Colombo, and J. Kim, “Characteristics of high-k al 2 o 3 dielectric using ozone-based atomic layer deposition for dual-gated graphene devices,” *Applied Physics Letters* **97**, 043107 (2010).
- ⁴¹S. Kim, J. Nah, I. Jo, D. Shahrjerdi, L. Colombo, Z. Yao, E. Tutuc, and S. K. Banerjee, “Realization of a high mobility dual-gated graphene field-effect transistor with al 2 o 3 dielectric,” *Applied Physics Letters* **94**, 062107 (2009).
- ⁴²I. J. Luxmoore, C. H. Gan, P. Q. Liu, F. Valmorra, P. Li, J. Faist, and G. R. Nash, “Strong coupling in the far-infrared between graphene plasmons and the surface optical phonons of silicon dioxide,” *ACS photonics* **1**, 1151–1155 (2014).
- ⁴³L. Falkovsky, “Optical properties of graphene,” in *Journal of Physics: Conference Series*, Vol. 129 (IOP Publishing, 2008) p. 012004.
- ⁴⁴G. T. Papadakis, *Optical Response in Planar Heterostructures: From Artificial Magnetism to Angstrom-Scale Metamaterials*, Ph.D. thesis, California Institute of Technology (2018).
- ⁴⁵A. Pochi Yeh, “Optical waves in layered media,” (1988).
- ⁴⁶Y. Nam, N. Lindvall, J. Sun, Y. W. Park, and A. Yurgens, “Graphene p–n–p junctions controlled by local gates made of naturally oxidized thin aluminium films,” *Carbon* **50**, 1987–1992 (2012).
- ⁴⁷M. H. Yusuf, B. Nielsen, M. Dawber, and X. Du, “Extrinsic and intrinsic charge trapping at the graphene/ferroelectric interface,” *Nano letters* **14**, 5437–5444 (2014).
- ⁴⁸S. Pendharker, H. Hu, S. Molesky, R. Starke-Bowes, Z. Poursoti, S. Pramanik, N. Nazemifard, R. Fedosejevs, T. Thundat, and Z. Jacob, “Thermal graphene metamaterials and epsilon-near-zero high temperature plasmonics,” *Journal of Optics* **19**, 055101 (2017).
- ⁴⁹P. N. Dyachenko, S. Molesky, A. Y. Petrov, M. Störmer, T. Krekeler, S. Lang, M. Ritter, Z. Jacob, and M. Eich, “Controlling thermal emission with refractory epsilon-near-zero metamaterials via topological transitions,” *Nature communications* **7**, 11809 (2016).
- ⁵⁰M. Lobet, B. Majerus, L. Henrard, and P. Lambin, “Perfect electromagnetic absorption using graphene and epsilon-near-zero metamaterials,” *Physical Review B* **93**, 235424 (2016).
- ⁵¹V. Veselago, “Soviet physics uspekhi, volume 10, number 4 january-february 1968.,” The Electrodynamics Of Substances With Simultaneously Negative values Of E And μ ” *PN Lebedev Physics Institute, Academy Of Sciences, USSR Usp. Fiz. Nauk* **92**, 517–526 (1964).
- ⁵²J. B. Pendry, “Negative refraction makes a perfect lens,” *Physical review letters* **85**, 3966 (2000).
- ⁵³M. Choi, S. H. Lee, Y. Kim, S. B. Kang, J. Shin, M. H. Kwak, K.-Y. Kang, Y.-H. Lee, N. Park, and B. Min, “A terahertz metamaterial with unnaturally high refractive index,” *Nature* **470**, 369 (2011).
- ⁵⁴V. P. Drachev, V. A. Podolskiy, and A. V. Kildishev, “Hyperbolic metamaterials: new physics behind a classical problem,” *Optics express* **21**, 15048–15064 (2013).
- ⁵⁵J. Zhou, T. Koschny, M. Kafesaki, E. Economou, J. Pendry, and C. Soukoulis, “Saturation of the magnetic response of split-ring resonators at optical frequencies,” *Physical review letters* **95**, 223902 (2005).
- ⁵⁶H. N. Krishnamoorthy, Z. Jacob, E. Narimanov, I. Kretzschmar, and V. M. Menon, “Topological transitions in metamaterials,” *Science* **336**, 205–209 (2012).
- ⁵⁷W. Gao, M. Lawrence, B. Yang, F. Liu, F. Fang, B. Béri, J. Li, and S. Zhang, “Topological photonic phase in chiral hyperbolic metamaterials,” *Physical review letters* **114**, 037402 (2015).
- ⁵⁸S. Tay, P.-A. Blanche, R. Voorakaranam, A. Tunç, W. Lin, S. Rokutanda, T. Gu, D. Flores, P. Wang, G. Li, *et al.*, “An updatable holographic three-dimensional display,” *Nature* **451**, 694 (2008).
- ⁵⁹J. Lutkenhaus, D. George, M. Moazzezi, U. Philipose, and Y. Lin, “Digitally tunable holographic lithography using a spatial light modulator as a programmable phase mask,” *Optics express* **21**, 26227–26235 (2013).
- ⁶⁰S. N. Khan and D. D. Johnson, “Lifshitz transition and chemical instabilities in ba 1- x k x fe 2 as 2 superconductors,” *Physical review letters* **112**, 156401 (2014).
- ⁶¹M. C. Rechtsman, J. M. Zeuner, Y. Plotnik, Y. Lumer, D. Podolsky, F. Dreisow, S. Nolte, M. Segev, and A. Szameit, “Photonic floquet topological insulators,” *Nature* **496**, 196 (2013).
- ⁶²Y. Li and J. Mei, “Double dirac cones in two-dimensional dielectric photonic crystals,” *Optics express* **23**, 12089–12099 (2015).
- ⁶³X. Huang, Y. Lai, Z. H. Hang, H. Zheng, and C. Chan, “Dirac cones induced by accidental degeneracy in photonic crystals and zero-refractive-index materials,” *Nature materials* **10**, 582 (2011).
- ⁶⁴S. Dai, Q. Ma, M. Liu, T. Andersen, Z. Fei, M. Goldflam, M. Wagner, K. Watanabe, T. Taniguchi, M. Thiemens, *et al.*, “Graphene on hexagonal boron nitride as a tunable hyperbolic metamaterial,” *Nature nanotechnology* **10**, 682 (2015).